Liao *et al. EURASIP Journal on Wireless Communications and Networking* (2019) 2019:144
https://doi.org/10.1186/s13638-019-1424-2

EURASIP Journal on Wireless Communications and Networking

RESEARCH Open Access

EKF/UKF-based channel estimation for robust and reliable communications in V2V and IIoT

Yong Liao[1], Xuanfan Shen[1], Guodong Sun[1], Xuewu Dai[2] and Shaohua Wan[3*]

Abstract

Cyber-physical systems (CPSs) are characterized by integrating computation, communication, and physical system. In typical CPS application scenarios, vehicle-to-vehicle (V2V) and Industry Internet of Things (IIoT), due to doubly selective fading and non-stationary channel characteristics, the robust and reliable end-to-end communication is extremely important. Channel estimation is a major signal processing technology to ensure robust and reliable communication. However, the existing channel estimation methods for V2V and IIoT cannot effectively reduce intercarrier interference (ICI) and lower the computation complexity, thus leading to poor robustness. Aiming at this challenge, according to the channel characteristics of V2V and IIoT, we design two channel estimation methods based on the Bayesian filter to promote the robustness and reliability of end-to-end communication. For the channels with doubly selective fading and non-stationary characteristics of V2V and IIoT scenarios, in the one hand, basis extended model (BEM) is used to further reduce the complexity of the channel estimation algorithm under the premise that ICI can be eliminated in the channel estimation. On the other hand, aiming at the non-stationary channel, a channel estimation and interpolation method based on extended Kalman filter (EKF) and unscented Kalman filter (UKF) Bayesian filters to jointly estimate the channel impulse response (CIR) and time-varying time domain autocorrelation coefficient is adopted. Through the MATLAB simulation, the robustness and reliability of end-to-end communication for V2V and IIoT are promoted by the proposed algorithms.

Keywords: CPS, V2V, IIoT, Channel estimation, Robustness, Reliability

1 Introduction

Cyber-physical systems (CPSs) are multidimensional complex systems with real-time perception, dynamic control, and information services, which consist of comprehensive computing, networking, and physical environments to implement information integration and deep collaboration using computing, communication, and control technologies (3Cs) [1–3]. CPS realizes the integrated design of computing, communication, and physical system, which can make the system more reliable and high efficient and realize real-time collaboration. Therefore, it has broad application prospects [4–6].

As an intelligent system, any problems in any link may affect the normal operation of the CPS, resulting in equipment damage, lower economic benefits, and even casualties. Thus, the stability of CPS, which is an enormous challenge in system design, should be considered and improved [4]. The stability of CPS mainly includes system reliability and robustness[1]. Firstly, to ensure the system reliability of operation, CPS should respond to the input of the system timely and effectively. In particular, for the auto-vehicle system (shown in Fig. 1) in the vehicle-to-vehicle (V2V) communication scenario, extremely high reliability for system communication is required [7]. Extremely demanding, traffic order and passenger safety are guaranteed only when the system can send the correct driving instructions to the target vehicle terminal quickly. Secondly, it is still necessary to ensure the system's robustness. In particular, for the process control system (shown in Fig. 2) in the Industry Internet of Things (IIoT) communication scenario, it requires extremely high robustness of system communication [8].

*Correspondence: shaohua.wan@ieee.org
[3]School of Information and Safety Engineering, Zhongnan University of Economics and Law, Wuhan 430073, China
Full list of author information is available at the end of the article

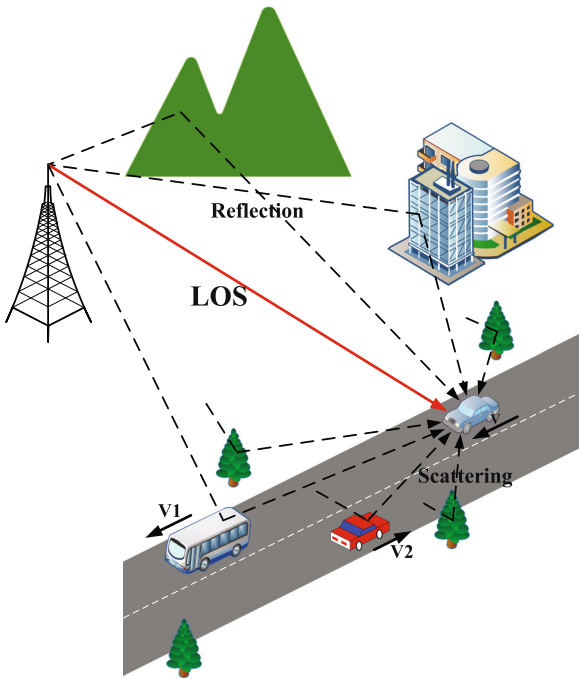

Fig. 1 The schematic diagram of V2V channel scene. This figure illustrates V2V communication scenario

With the movement of the terminal, the channel state may change drastically in a short period of time, and the electromagnetic environment in the factory is complicated. So, the system should be able to effectively complete the data transmission in the case of frequently switching of the channel state.

At the communication system receiver, channel estimation plays an important role in improving the reliability and robustness of the communication system in different communication scenarios. The pilot symbols are firstly utilized to obtain the channel impulse response (CIR) of the partial frequency or time in channel estimation, and then, the channel interpolation method is used to calculate the channel response of the entire time-frequency domain resource block [9]. Finally, the estimated channel response for channel equalization is utilized to eliminate the wireless signal distortion and interference introduced by the channel during signal propagation. Therefore, in order to improve the reliability and robustness of CPS, the physical channel features of the V2V and IIoT should be analyzed and studied. The V2V communication scenario is shown in Fig. 1. Because the terminal is in the state of high-speed movement, the channel will exhibit the selective fading (doubly selective fading) in the time-frequency domain under the combination of multipath effect and the Doppler effect [7, 10]. At the same time, some recent studies have pointed out that the time-domain autocorrelation coefficient of the CIR appears time-varying or non-stationary characteristics due to the rapidly time-varying characteristics of the geometric parameters of the beam between the receiving antenna array and the base station. For the IIoT scenario shown in Fig. 2, due to the influence of various scatters in the factory, the number of taps of the channel is time-varying [8, 11]. It means that the transmission path of the wireless channel includes not only a direct path but also scatter paths and dynamic paths. Therefore, the time domain autocorrelation function of the channel also exhibits time-varying characteristics. At the same time, in the communication scenario of IIoT, since the scatters in the factory are very rich and in moving states, the channel will also show the doubly selective fading characteristics.

According to the form of its estimated channel response, the channel estimation methods can be classified into the time domain and frequency domain channel estimations, respectively. It is worthy mentioning that the methods of time domain channel estimation can effectively eliminate the intercarrier interference (ICI) in the channel estimation because the CIR is estimated directly. Since this paper is aimed at the scenario of the doubly selective fading channel that may exist severe ICI, the time domain channel estimation method is adopted. Moreover, the basis expansion model (BEM) can effectively reduce the complexity of the estimation by transforming the CIR to a low dimensional space formed by the base vector. At the same time, the damage of the channel information can be almost ignored by the selection of a reasonable base vector. Consequently, the BEM has been widely applied in channel estimation for doubly selective channels [10, 12].

In view of the non-stationary characteristics of the channel, based on Bayesian filter, our previous research results have pointed out that the joint estimation of the CIR and the time domain autocorrelation coefficient of time-varying channel is an effective method for tracking the response changes of non-stationary channels.

In our previous research [13], a non-stationary channel estimation method based on extended Kalman filter (EKF) is proposed. However, the method is limited by its model and cannot effectively deal with ICI. Therefore, the estimation accuracy is low and it is not applicable to communication scenarios such as V2V or IIoT.

In summary, in order to improve the robustness and reliability of the end-to-end communication link of CPS, channel estimation and interpolation is implemented based on Bayesian filtering and the theories of BEM, joint estimation of channel response, and time domain correlation coefficient. Finally, the accuracy of channel estimation and the ability of combat complex and variable communication environments could be improved.

The main contributions of this paper are as follows:

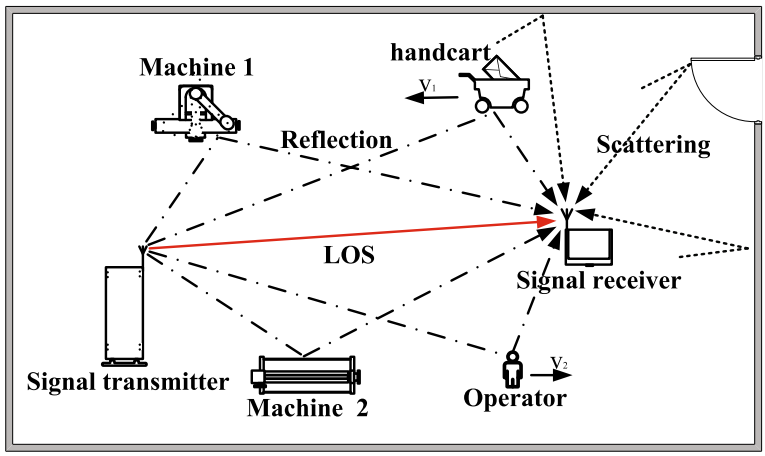

Fig. 2 The schematic diagram of IIoT channel scene. This figure illustrates the IIoT communication scenario

1. For the channels with doubly selective fading characteristics of V2V and IIoT scenarios in CPS, BEM is used to further reduce the complexity of the channel estimation algorithm under the premise that ICI can be eliminated in the channel estimation.

2. Based on the non-stationary characteristics of the channels in V2V and IIoT scenarios, this paper uses channel estimation and interpolation method based on EKF and unscented Kalman filter (UKF) Bayesian filters to jointly estimate the CIR and time-varying time domain autocorrelation coefficients.

3. The system complexity of the proposed algorithms is further analyzed. Due to the fact that the BEM is utilized, the CIR matrix is transformed from N dimension to QL dimension ($QL \ll N$), where N is the number of subcarriers, Q and L denote the dimension of basis vector and the number of taps, respectively. Thus, the complexity of the channel estimation algorithms including least square (LS), EKF, and UKF is greatly reduced.

4. Through the MATLAB simulation platform, we compare the normalized minimum mean error (NMSE) and bit error rate (BER) performance of the LS, EKF, and UKF BEM-based channel estimation algorithms at different terminal moving velocity in the V2V scene, as well as the NMSE and BER performance under the condition of different taps in the IIoT scene. The mean and variance of the BER are listed under the conditions of different channel estimation algorithms at different terminal moving speeds and taps. Simulation results show that the proposed channel estimation methods could be applied to V2V and IIoT scenarios to promote the robustness and reliability of end-to-end communication.

The rest of this paper is organized as follows. In Section 2, the related works are presented and analyzed. In Section 3, both the system model and channel model are presented. In Section 4, we propose the BEM-EKF and BEM-UKF channel estimation methods, including state space model, updating equation, and analyzing of complexity. In Section 5, the performances of the proposed methods are compared with the traditional methods in V2V and IIoT environments by MATLAB. Finally, the conclusion is discussed in Section 6.

2 Related work

2.1 The robust communications in V2V

For the past few years, the Internet of Vehicle (IoV) communication has successfully verified its superiority in various fields. In order to improve traffic safety by adopting advanced wireless communication systems, further investigations and studies on V2V are carried out widely. Based on the channel measurement method, literatures [14] and [15] show that the V2V channel is time-varying and non-stationary due to the mobility of the transmitter/receiver terminal or the existence of dynamic scatters. Thus, setting up future measurement campaigns and proposing more realistic V2V channel models are the two challenges. To ensure frequency non-selectivity and minimum ICI, the performance analysis of orthogonal frequency division multiplexing (OFDM)-based V2V communication system is reported in [16], which aims to alleviate the Doppler spread of vehicles when driving at high speed. Time variation and its time-frequency domain selectivity of channel, which lead to non-stationarity characteristic, are further discussed in [17], and the non-stationarity characteristic of V2V channels is one of the key factors that must be considered in establishing a correct channel model. In order to take advantage of upcoming V2V applications, a robust method of communication between vehicles must

be established. Literature [18] points out that the main challenge of V2V communication system is the robustness of the entire communication system caused by extremely fast time-varying channel characteristics in high speeds and the high mobility of the environment. Therefore, the channel response of the system must be accurately estimated before it can be used for equalization, demodulation, and decoding. Thus, accurate and reliable channel estimation is critical to the overall system performance. In [19], a channel estimation scheme is proposed by constructing pilots using the data symbols and properly exploiting the correlation characteristics of V2V channels. Three different Doppler shifts in the vehicle networking environment are compared by using simulation, which proves that the proposed constructed data pilot (CDP) estimation scheme has a good robustness, especially in high signal-to-noise ratio (SNR) regime. The method for reducing the complexity associated with the estimation and equalization of a doubly selective channel is proposed in [20]. However, it will reduce the system robustness. Meanwhile, the author also proposes a new algorithm of Gradient Rake-Matching Pursuit (GRMP) algorithm to reduce complexity and improve system robustness. Three channel estimation and tracking algorithms, Finite Alphabet with Time Truncation (FA-TT), Minimum Distance with Time Truncation (MD-TT), and Decision Directed with Time Truncation (DD-TT) are reposted in [21]. Those algorithms obtain very high performance in low mobile environments as well as fast varying channels, which meet the requirements of improving system robustness. In [22], non-stationary channel models based on the well-known tapped delay line (TDL) model are used; the authors compare the BER performance of different channel interpolation algorithms at different moving speeds, which reveals that the robustness can be further improved since the performance degradation from the optimum performance is still significant.

2.2 The robust communications in IIoT

In recent years, in addition to the IoV, wireless communication and networking have been introduced into industrial systems due to the advantage of cable-free deployment [23]. Because of the presence of significant noise and interference effects caused by large machinery and heavy multipath propagation effects caused by highly reflective structures [24], the performance of the wireless channel in an industrial environment are different with the radio channels in home and office environments. In order to avoid the problems of industrial equipment damage, security risks and economic losses due to the instability of the wireless network, the approaches to improve the stability and reliability of the wireless network are urgent. The studies on the fading channel in industrial scenarios last over decades. Measurement-based approach examining the fading effect of the factories environment are reported in [25, 26], and the results identify that the industrial channel still follows the classical propagation principle and the existence of heavy temporal fading effect. The work in [27] attempts to model the time variant mobile peer-to-peer fading effect with the extension to the classical mobile channel model. A state of the art survey on the industrial fading channel has been provided in [24], which confirms the temporal fading effects. Since doubly selective or time-varying multipath channels caused by the propagation channel environment of IIoT will affect the robustness of the entire communication system [20]. In addition, since the channel state is varying and the equalizer must be constantly updated to match the channel changing, it is difficult to realize estimation and equalization simultaneously [28, 29]. A low-complexity channel estimation scheme based on compressed sensing in IIoT environment is proposed in [20], and the simulations results show that the proposed method can effectively improve the robustness of the system.

3 System model

With the rapid development of communication technology, people are pursuing high-speed and stable wireless data transmission. At the same time, the shortage of frequency band resources is becoming more and more serious. The OFDM communication system uses multicarrier modulation to improve the data transmission rate and effectively combat the influence of multipath fading, and the positive subcarrier modulation greatly improves the utilization rate of the frequency band. It can be seen that the OFDM system satisfies the needs of modern wireless communication technology. The IEEE 802.11p protocol used in the V2V and the IEEE 802.15.4 protocol commonly used in the IIoT all use the block pilot insertion [30, 31]. Therefore, we use the OFDM communication system based on block pilot as the basis of the research as shown in Fig. 3.

Considering an OFDM system with N subcarriers, there are I OFDM symbols in a subframe. $s_i(n)$ is defined as a transmitted symbol at ith OFDM symbol on nth subcarrier, and the vector of transmitted symbols at ith OFDM symbol is $\mathbf{s}_i = [s_i(0), \ldots, s_i(N-1)]^{\mathrm{T}}$. The OFDM modulation for $\mathbf{s}_i$, inverse discrete Fourier transforming (IDFT), can be expressed as

$$\mathbf{S}_i = \mathbf{F}^{\mathrm{H}} \mathbf{s}_i \tag{1}$$

where $\mathbf{S}_i = [S_i(0), \ldots, S_i(N-1)]^{\mathrm{T}}$ is the transmitted sequences in time domain and $[\mathbf{F}]_{n,k} = \frac{1}{\sqrt{N}} \exp\left(-j\frac{2\pi}{N}kn\right)$ is the Fourier transforming matrix. Then, the OFDM communication model can be described as

$$\mathbf{y}_i = \mathbf{H}_i \mathbf{s}_i + \mathbf{z}_i \tag{2}$$

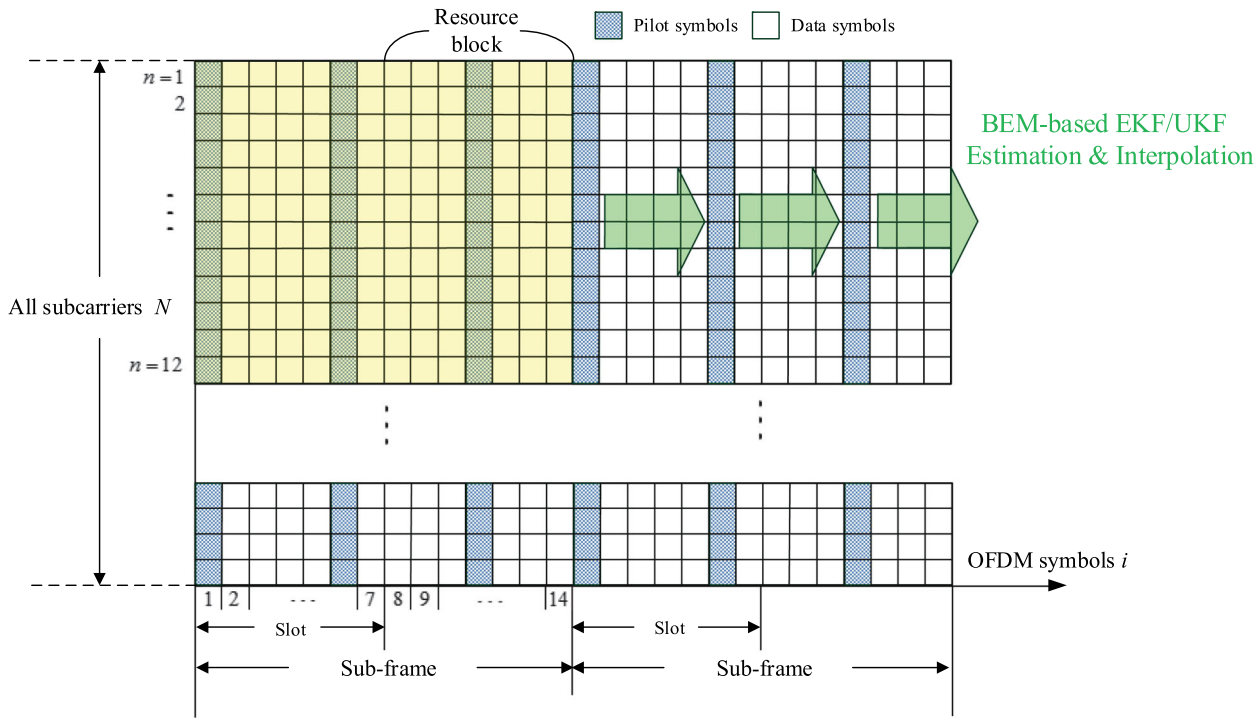

Fig. 3 Frame structure and pilot pattern. OFDM communication system based on block pilot satisfies the needs of modern wireless communication technology

where $\mathbf{y}_i = \left[y_i(0), \ldots, y_i(N-1)\right]^{\mathrm{T}}$ is the vector of received symbols at the ith OFDM symbol, $\mathbf{z}_i$ is an additive complex Gaussian noise with zero mean, and covariance matrix $\mathbf{Q}_z = \sigma_z^2 \mathbf{I}_N$, where the σ_z^2 is variance of $\mathbf{z}_i$, and $\mathbf{H}_i \in \mathbb{C}^{N\times N}$ denotes the channel frequency response (CFR) matrix at ith OFDM symbol, which could be described by the CFR matrix as

$$\mathbf{H}_i = \mathbf{F}\mathbf{g}_i\mathbf{F}^{\mathrm{H}} \tag{3}$$

where the $\mathbf{g}_i \in \mathbb{C}^{N\times N}$ is the CIR matrix at ith OFDM symbol

$$\mathbf{g}_i = \begin{bmatrix} h_i(0,0) & 0 & \cdots & h_i(0,L-1) & \cdots & h_i(0,1) \\ h_i(1,1) & h_i(1,0) & 0 & \cdots & \cdots & h_i(1,2) \\ \vdots & \ddots & \ddots & \ddots & \ddots & \vdots \\ 0 & \cdots & 0 & h_i(N-1,L-1) & \cdots & h_i(N-1,0) \end{bmatrix}$$

where the $h_i(k,l)$ is the kth CIR sample point on lth tap at ith OFDM symbol.

Under the doubly selective channel condition, the frequency domain channel estimation methods cannot eliminate ICI, and the time domain channel estimation methods can effectively eliminate the impact of ICI by directly estimating the CIR. However, the time domain channel estimation needs a complete CIR in a symbolic time, which greatly increases the number of parameters to be estimated. Therefore, the BEM is adopted to reduce the space complexity of channel estimation. For the BEM channel model, the selection of base vectors is the key issue. According to the difference of base vectors, the BEM channel model also includes complex exponential BEM (CE-BEM), prolate spheroidal BEM (PS-BEM), Karhunen-Loeve BEM (KL-BEM), and polynomial BEM (P-BEM) [32]. Because the base vectors of CE-BEM are easy to acquire, which does not depend on additional channel statistical information, and they are pairwise orthogonal, the CE-BEM is chosen as the basic channel model in this paper.

Assuming that the number of taps of multi-path channel is L, the CIR could be described by CE-BEM as

$$h_i(k,l) = \sum_{q=0}^{Q-1} b_{k,q} c_{i,l}^{q} = \mathbf{b}_k^{\mathrm{T}} \mathbf{c}_{i,l} \tag{4}$$

where Q is the dimension of base vectors ($Q \ll N$) and $\mathbf{b}_k = \left[b_{k,0}, \ldots, b_{k,Q-1}\right]^{\mathrm{T}}$ is the kth base vector and $b_{k,q} = \exp\left(\frac{j2\pi(q-Q)k}{N}\right)$. Due to the fact that the CE-BEM is adopted, $\mathbf{c}_{i,l} = \left[c_{i,l}^{(0)}, \ldots, c_{i,l}^{(Q-1)}\right]^{\mathrm{T}}$ is the vector of coefficients of BEM. Let $\mathbf{h}_{i,l} = [h_i(0,l), \ldots, h_i(N-1,l)]^{\mathrm{T}}$ denote the vector of CIR on lth tap at ith OFDM symbol, and the vector of CIR at ith OFDM symbol $\mathbf{h}_i$ could be described as

$$\mathbf{h}_i = \left[\mathbf{h}_{i,0}^{\mathrm{T}}, \ldots, \mathbf{h}_{i,L-1}^{\mathrm{T}}\right]^{\mathrm{T}} = \mathbf{B}\mathbf{c}_i \tag{5}$$

where $\mathbf{B} = \mathbf{I}_L \otimes [\mathbf{b}_0, \ldots, \mathbf{b}_{N-1}]^{\mathrm{T}}$, $\mathbf{c}_i = \left[\mathbf{c}_{i,0}^{\mathrm{T}}, \ldots, \mathbf{c}_{i,L-1}^{\mathrm{T}}\right]^{\mathrm{T}}$.

Then, the BEM-based base-band OFDM communication model could be expressed as

$$\mathbf{y}_i = \mathbf{A}_i \mathbf{c}_i + \mathbf{z}_i \tag{6}$$

where $\mathbf{A}_i$ denotes the measurement matrix as

$$\mathbf{A}_i = \mathbf{F}\tilde{\mathbf{S}}_i\mathbf{B} \tag{7}$$

where $\tilde{\mathbf{S}}_i$ is consisted by transmitted symbols from transmitter, as

$$\tilde{\mathbf{S}}_i = \left[\mathbf{S}_i^{(0)}, \ldots, \mathbf{S}_i^{(L-1)}\right] and \mathbf{S}_i^{(l)} = diag\left\{\left[S\left(N-l\right), S\left(N-l+1\right), \ldots, S\left(0\right), \ldots, S\left(N-l-1\right)\right]\right\}$$

.

Then, we could construct a time-varying auto regression (TVAR) model for BEM-based CIR as

$$\mathbf{c}_{i+1} = \mathbf{R}_i \mathbf{c}_i + \mathbf{v}_i \tag{8}$$

where $\mathbf{R}_i$ is the correlation matrix of the coefficients of BEM for adjacent OFDM symbols, $\mathbf{v}_i$ is the process noise with variance σ_v^2 , and covariance matrix $\mathbf{Q}_v = \sigma_v^2 \mathbf{I}_{QL}$. It could be concluded from [33] that $\mathbf{R}_i$ is obtained by mapping the time domain correlation coefficient matrix of the CIR to a linear space based on the base matrix $\mathbf{B}$. Because the base vectors of CE-BEM model are pairwise orthonormal, it can be considered that the CE-BEM entirely eliminates the time correlation of the CIR on base space, which means that the coefficients of BEM are pairwise uncorrelated. Based on that, we could consider $\mathbf{R}_i$ as a diagonal matrix, and the elements on the diagonal are the correlation coefficients of the BEM coefficients.

4 Channel estimation and interpolation

The challenge of estimation and interpolation in time domain for non-stationary channel would be coped with an EKF or UKF, which could jointly estimate the CIR and channel time correlation coefficients.

4.1 State space model

In order to jointly estimate the coefficients of BEM $\mathbf{c}_i$ and the channel time correlation coefficients $\mathbf{R}_i$, we redefine a correlation coefficients vector $\mathbf{r}_i$ with the diagonal elements of $\mathbf{R}_i$ as

$$\mathbf{r}_i = vec\left(\mathbf{R}_i\right). \tag{9}$$

According to [13], assuming a random walk model for $\mathbf{r}_i$, the state space model can be constructed as

$$\begin{cases} \mathbf{r}_{i+1} = \mathbf{r}_i + \mathbf{w}_i \\ \mathbf{c}_{i+1} = \mathbf{R}_i \mathbf{c}_i + \mathbf{v}_i \\ \mathbf{y}_i = \mathbf{A}_i \mathbf{c}_i + \mathbf{z}_i \end{cases} \tag{10}$$

where $\mathbf{w}_i$ denotes process noise of time correlation coefficients $\mathbf{r}_i$ and it is an independent zero-mean Gaussian complex white noises, with covariance matrix $\mathbf{Q}_w = \sigma_w^2 \mathbf{I}_{QL}$, where σ_w^2 is the variance of $\mathbf{w}_i$. Then, a new state variable can be defined as $\mathbf{x}_i = \left[\mathbf{r}_i \ \mathbf{c}_i\right]^{\mathrm{T}}$, and the state space model can be further derived as

$$\begin{cases} \mathbf{x}_{i+1} = f\left(\mathbf{x}_i\right) + \mathbf{u}_i \\ \mathbf{y}_i = \left[\mathbf{0} \ \mathbf{A}_i\right]\mathbf{x}_i + \mathbf{z}_i \end{cases} \tag{11}$$

where $f\left(\mathbf{x}_i\right) = \begin{bmatrix} \mathbf{r}_i \\ \mathbf{R}_i\mathbf{c}_i \end{bmatrix} = \begin{bmatrix} \mathbf{r}_i \\ diag\left(\mathbf{r}_i\right)\mathbf{c}_i \end{bmatrix}$ is a nonlinear state transform equation.

4.2 EKF

Applying the principle of EKF, we could get a linear state space model by the first order Taylor approximation as

$$\begin{cases} \mathbf{x}_{i+1} = \mathbf{T}_i \mathbf{x}_i + \mathbf{u}_i \\ \mathbf{y}_i = \left[\mathbf{0} \ \mathbf{A}_i\right]\mathbf{x}_i + \mathbf{z}_i \end{cases} \tag{12}$$

where $\mathbf{T}_i = \begin{bmatrix} \mathbf{I}_{QL} & \mathbf{0} \\ \frac{1}{2}\hat{\mathbf{C}}_i & \frac{1}{2}\hat{\mathbf{R}}_i \end{bmatrix}$ is state transform matrix of $\mathbf{x}_i$, $\hat{\mathbf{C}}_i$=diag $\left(\hat{\mathbf{c}}_i\right)$ is a diagonal matrix consist of the *a posterior* estimates of the coefficients of BEM, $\hat{\mathbf{R}}_i$ is the a posterior time correlation coefficients matrix, and $\mathbf{u}_i$ is the process noise vector of state transfer equation with the covariance matrix $\mathbf{Q}_u = \begin{bmatrix} \mathbf{Q}_w & \mathbf{0} \\ \mathbf{0} & \mathbf{Q}_v \end{bmatrix}$.

In the state prediction process, it is necessary to make a prediction of the a priori estimates of the state variable at the next moment based on the *a posterior* estimates, which is estimated at the previous moment with state transfer equations, and the state prediction equations can be described as

$$\mathbf{x}_{i|i-1} = \mathbf{T}_{i-1}\mathbf{x}_{i-1} \tag{13}$$

$$\mathbf{P}_{i|i-1} = \mathbf{T}_{i-1}\mathbf{P}_{i-1}\mathbf{T}_{i-1}^{\mathrm{T}} + \mathbf{Q}_u \tag{14}$$

where $\mathbf{P}_{i|i-1}$ denotes the a priori covariance matrix of ith state variable.

As mentioned above, the measurement matrix of data symbols are difficult to acquire. Here, we propose a decision-directed scheme to construct the measurement matrix as follows. Predicted CIR vector $\mathbf{h}_{i|i-1}$ can be obtained from the a priori coefficients of BEM $\mathbf{c}_{i|i-1}$ by (5) at first, and then, it can be transformed into a priori CFR matrix $\mathbf{H}_{i|i-1}$ by (3). Therefore, the transmitted symbols vector $\mathbf{s}_i$ of ith OFDM symbol can be calculated through the MMSE equalization as

$$\hat{\mathbf{s}}_i = \left(\mathbf{H}_{i|i-1}^{\mathrm{H}}\mathbf{H}_{i|i-1} + \sigma_z^2\mathbf{I}_N\right)^{-1}\mathbf{H}_{i|i-1}^{\mathrm{H}}\mathbf{y}_i \tag{15}$$

where $\hat{\mathbf{s}}_i$ denotes the predicted value of transmitted symbols vector. However, $\hat{\mathbf{s}}_i$ might deviate from the original constellation points of transmitted symbols $\mathbf{s}_i$ due to the influence of noise and the error of channel state prediction. Obviously, measurement matrix constructed by $\hat{\mathbf{s}}_i$

is inappropriate, a decision-directed scheme is proposed herein to improve the validity of state measurement.

The operation of decision-directed scheme is described in detail as follows. The modulation symbol set of transmitted symbols is defined as $\mathbf{S}=\{S_0,...,S_{M-1}\}$, where S_m denotes the one of the modulation symbols and $\log_2 M$ is the modulation order. The output of decision-directed scheme $\hat{s}_i^{(d)}(n)$ is the modulation symbol which is the nearest one for $\hat{s}_i(n)$, as

$$\hat{s}_i^{(d)}(n)=\min_{S_m\in\mathbf{S}}\left\|S_m-\hat{s}_i(n)\right\|. \tag{16}$$

Thus, the measurement matrix $\hat{\mathbf{A}}_i^{(d)}$ can be constructed from $\hat{\mathbf{s}}_i^{(d)}$ by (7), and it could be put into the state update equations of EKF.

In this situation that the received signal is affected by noise significantly, the decision error $\hat{\mathbf{s}}_i^{(d)}$, which $\hat{\mathbf{s}}_i^{(d)}\neq\mathbf{s}_i$, would lead to an obvious measurement error which would propagate with the iteration of EKF until next pilot symbol arrived. Nevertheless, the decision-directed scheme is very simple, and the cost of hardware implementation for decision-directed scheme is low.

After state prediction, the a posterior state variable $\mathbf{x}_i$ would be estimated through the state updating equations of EKF as

$$\mathbf{K}_i=\mathbf{P}_{i|i-1}\begin{bmatrix}\mathbf{0}\\ \mathbf{A}_i^{\mathrm{H}}\end{bmatrix}\left(\begin{bmatrix}\mathbf{0} & \mathbf{A}_i\end{bmatrix}\mathbf{P}_{i|i-1}\begin{bmatrix}\mathbf{0} & \mathbf{A}_i\end{bmatrix}^{\mathrm{T}}+\mathbf{Q}_z\right)^{-1} \tag{17}$$

$$\mathbf{x}_i=\mathbf{x}_{i|i-1}+\mathbf{K}_i\left(\mathbf{y}_i-\begin{bmatrix}\mathbf{0} & \mathbf{A}_i\end{bmatrix}\mathbf{x}_{i|i-1}\right) \tag{18}$$

$$\mathbf{P}_i=\mathbf{P}_{i|i-1}-\mathbf{K}_i\begin{bmatrix}\mathbf{0} & \mathbf{A}_i\end{bmatrix}\mathbf{P}_{i|i-1} \tag{19}$$

where $\mathbf{K}_i$ is the gain of EKF. It is worth mentioning that the complexity would be increased because of the matrix inversing in (17). However, BEM is used to establish the state space model of EKF, the relationship between the complexity and estimation accuracy can be effectively controlled by adjusting the compression base vector dimension Q according to the actual application scenario.

4.3 UKF

The UKF uses a deterministic sampling technique known as the unscented transform (UT) to pick a minimal set of sample points (called sigma points) around the mean. The sigma points are propagated through the nonlinear functions, from which a new mean and covariance estimate are formed. There are three main steps for the state prediction of UKF, including generating of sigma points, substituting the sigma points into the transformation equation, and calculating the means of the a priori state variable and covariance matrix.

According to the length of the vector of state variable, the number of sigma points should be set as $2QL+1$. The a posterior sigma points could be described as

$$\begin{aligned}\chi_{i-1}^{(0)}&=\mathbf{x}_{i-1}\\ \chi_{i-1}^{(j)}&=\mathbf{x}_{i-1}+\sqrt{QL+\lambda}\left[\sqrt{\mathbf{P}_{i-1}}\right]_j\\ \chi_{i-1}^{(QL+j)}&=\mathbf{x}_{i-1}-\sqrt{QL+\lambda}\left[\sqrt{\mathbf{P}_{i-1}}\right]_j\ (j=1,\ldots,QL)\end{aligned} \tag{20}$$

where $\chi_{i-1}^{(j)}$ denotes the jth sigma point, $\mathbf{x}_{i-1}$ is the a posterior estimate of state variable on the $(i-1)$th OFDM symbol, $\mathbf{P}_{i-1}$ denotes the a posterior covariance matrix on the $(i-1)$th OFDM symbol, and the λ is the weight factor of covariance

$$\lambda=\alpha^2(QL+\beta)-QL \tag{21}$$

where α and β control the spread of the sigma points. According to the state space model proposed in (11) and the parameters setting recommendation for UKF in [34], we set the α as 0.95 and β as 2, respectively. The sigma points are propagated through the transition function

$$\hat{\chi}_i^{(j)}=f\left(\hat{\chi}_{i-1}^{(j)}\right),j=0,...,2QL \tag{22}$$

where the $\hat{\chi}_i^{(j)}$ is the predicted sigma points. The weighted sigma points are recombined to produce the predicted state and covariance, which can be derived as

$$\mathbf{x}_{i|i-1}=\sum_{j=0}^{2QL}W_j^{(m)}\hat{\chi}_i^{(j)} \tag{23}$$

$$\mathbf{P}_{i|i-1}=\sum_{j=0}^{2QL}W_j^{(c)}\left(\hat{\chi}_i^{(j)}-\mathbf{x}_{i|i-1}\right)\left(\hat{\chi}_i^{(j)}-\mathbf{x}_{i|i-1}\right)^{\mathrm{T}}+\mathbf{Q}_v \tag{24}$$

where $W_j^{(m)}$ and $W_j^{(c)}$ are the weights of state and covariance, which are given by

$$\begin{aligned}W_0^{(c)}&=\tfrac{\lambda}{QL+\lambda}\\ W_0^{(m)}&=\tfrac{\lambda}{QL+\lambda}+\left(1-\alpha^2+\beta\right)\\ W_j^{(c)}&=W_j^{(m)}=\tfrac{1}{2(QL+\lambda)}\ (j=1,\ldots,2QL)\end{aligned} \tag{25}$$

In the next step, the predicted state $\mathbf{x}_{i|i-1}$ and covariance $\mathbf{P}_{i|i-1}$ are utilized to calculate the a posterior state and covariance which would be fed to the equalizer and demodulator.

The a posterior estimates of state variable would be calculated by updating equations according to the a priori estimates. There are four steps in the program of state updating: generating of sigma points; substituting the sigma points into the measurement equation; calculating the mean, covariance matrix, and cross-covariance matrix of measurement variable; and computing the gain of filtering and the a posterior estimates and covariance matrix of state variable, respectively.

There are also $2QL+1$ a priori sigma points would be generated as

$$\begin{aligned}\chi_{i|i-1}^{(0)} &= \mathbf{x}_{i|i-1}\\ \chi_{i|i-1}^{(j)} &= \mathbf{x}_{i|i-1} + \sqrt{QL+\lambda}\left[\sqrt{\mathbf{P}_{i|i-1}}\right]_j\\ \chi_{i|i-1}^{(j+QL)} &= \mathbf{x}_{i|i-1} - \sqrt{QL+\lambda}\left[\sqrt{\mathbf{P}_{i|i-1}}\right]_j (j=1,\ldots,QL)\end{aligned} \quad (26)$$

The decision-directed method is utilized to construct the measurement matrix $\hat{\mathbf{A}}_i$, so we would obtain the measurement sigma points by substituting the sigma points into the measurement equation like

$$\hat{\gamma}_i^{(j)} = \left[\mathbf{0}\ \hat{\mathbf{A}}_i\right]\chi_{i|i-1}^{(j)}\ (j=0,\ldots,2QL) \quad (27)$$

where $\hat{\gamma}_i^{(j)}$ denotes the jth measurement sigma point on the ith OFDM symbol. The weighted a priori sigma points are recombined to produce the mean, covariance matrix, and cross-covariance matrix of $\hat{\gamma}_i^{(j)}$ as

$$\mu_i = \sum_{j=0}^{2QL} W_j^{(m)}\hat{\gamma}_i^{(j)} \quad (28)$$

$$\mathbf{T}_i = \sum_{j=0}^{2QL} W_j^{(c)}\left(\hat{\gamma}_i^{(j)}-\mu_i\right)\left(\hat{\gamma}_i^{(j)}-\mu_i\right)^{\mathrm{T}} + \mathbf{Q}_w \quad (29)$$

$$\mathbf{C}_i = \sum_{j=0}^{2QL} W_j^{(c)}\left(\chi_{i|i-1}^{(j)}-\mathbf{x}_{i|i-1}\right)\left(\hat{\gamma}_i^{(j)}-\mu_i\right)^{\mathrm{T}} \quad (30)$$

where μ_i is the mean of measurement sigma points, $\mathbf{T}_i$ is the covariance matrix, and $\mathbf{C}_i$ is the cross-covariance matrix.

Then, the gain of filtering $\mathbf{K}_i$, the a posterior estimates $\mathbf{x}_i$ and the covariance matrix $\mathbf{P}_i$ could be described as

$$\mathbf{K}_i = \mathbf{C}_i\mathbf{T}_i^{-1} \quad (31)$$

$$\mathbf{x}_i = \mathbf{x}_{i|i-1} + \mathbf{K}_i\left(\mathbf{y}_i-\mu_i\right) \quad (32)$$

$$\mathbf{P}_i = \mathbf{P}_{i|i-1} - \mathbf{K}_i\mathbf{T}_i\mathbf{K}_i^{\mathrm{T}}. \quad (33)$$

4.4 System complexity

Table 1 showed the comparison of the computational complexity (the number of times) for several classical channel estimation methods, similar channel estimation methods, and the proposed BEM-based EKF and BEM-based UKF methods in an OFDM symbol.

Table 1 The mean for BEM-based channel estimation methods in different velocity

Velocities (km/h)	LS	EKF	UKF
0	0.0712	0.0152	0.0148
30	0.0732	0.0174	0.0165
60	0.0768	0.0202	0.0185
90	0.0803	0.0238	0.0210
120	0.0874	0.0329	0.0295
150	0.0933	0.0389	0.0333

The LS, EKF, and UKF methods in Table 1 all belong to frequency channel estimation method without BEM. It could be also witnessed that the complexity of BEM-based channel estimation methods is based on the dimension of basis vector Q and the number of taps L, rather than the number of subcarriers N. Generally, the $QL \ll N$, so the complexity of BEM-based methods is much lower than frequency channel estimation.

Compared with the BEM-based LS method, the complexity of the BEM-based EKF is about 5 times of it, but both of them are still in a same level. According to the (22) and (27), we find that the main part of the complexity of the BEM-based UKF method is substituting the sigma points into the measurement equation and transforming equation, because the times of substituting sigma points depend on the number of sigma points and the calculation of substituting for all sigma point is $(2QL+1)\ (QL)^3$. Although the complexity of BEM-based UKF is in a higher level than the BEM-based EKF and the BEM-based LS, the BEM could ensure it keeps in a reasonable value. And the performances of these methods in both V2V and IIoT scenarios will be presented in the next section.

5 Experimental design

In this section, we would like to present and compare the performances of the BEM-EKF and BEM-UKF with traditional channel estimation methods in V2V and IIoT environments. Firstly, the simulation parameters are presented, and the simulation results of the methods proposed in this paper are analyzed. Particularly, for demonstrating and showing the robustness and reliability of the end-to-end communication systems with BEM-EKF and BEM-UKF in CPS, we pay more attention to observe and analyze the simulation results in some environments, including the V2V environments with high velocity and the IIoT environments with very deep doubly selective fading.

5.1 Simulation parameters

The NMSE and BER performances of BEM-LS as well as BEM-EKF and BEM-UKF proposed in this paper are simulated by MATLAB, and the results are compared and analyzed as follows. Actually, for simulating the most general end-to-end communication in V2V and IIoT environments, we set the basic parameters of end-to-end communication system as the definition in LTE [35] which is one of the common and available physical layer communication protocols for both V2V and IIoT. The parameters of end-to-end OFDM communication system are shown in Table 2 . It is worth mentioning that the setting about the variance of process noise σ_w^2 and σ_v^2, according to (8) and (10), the σ_w^2 and σ_v^2 present the uncertainty of the

Table 2 The variance for BEM-based channel estimation methods in different velocity

Velocities (km/h)	LS	EKF	UKF
0	6.1436e−05	2.4785e−06	2.7124e−06
30	3.9089e−04	3.2700e−04	2.3728e−04
60	5.3562e−04	3.8719e−04	3.1166e−04
90	3.8699e−04	3.6670e−04	2.2423e−04
120	4.1918e−04	3.6670e−04	2.1158e−04
150	4.1834e−04	3.8870e−04	1.4793e−04

Table 4 The variance for BEM-based channel estimation methods in different taps

Number of taps	LS	EKF	UKF
3	9.4563e−04	7.9185e−04	6.5175e−04
6	4.6187e−04	3.8377e−04	3.3921e−04
9	5.4519e−04	4.3288e−04	3.3844e−04
12	5.7751e−04	2.8968e−04	2.5852e−04
15	3.4490e−04	1.4435e−04	1.3037e−04
18	4.4029e−04	1.8785e−04	1.8235e−04

prediction for CIR and the range of variation of time coefficient. According to [10], the most appropriate way to get the values of them is to measure and track the accurate changing of physical channel parameters, including direction of arrival (DoA) and so on, but it is really difficult and complex to get them. Then, in our previous research [36], the variance of process noise is set as a reasonable constant after some adjusting, and we demonstrated that it is a kind of effective and simple way to cope with this problem, so we did the same work in this paper and set them as follows.

As mentioned above, the robustness and reliable performances of communication system in V2V and IIoT environments are what we focus on in this paper, so the basic parameters for V2V and IIoT physic wireless channel are very important and they are presented in Tables 3 and 4.

For V2V environments, the CPS with high robustness and reliable should be able to work in situations with different velocities. According to the extended vehicle model (EVM) defined by LTE, we set the multi-path channel parameters, including the information about taps and fading type, as follows. Then, considering the V2V environments with very high terminal speed are always occurred in expressway where the multi-path effect is not obvious and the line of sight (LoS) should not be neglected, so the Rician channel model is chosen to be the fading type of V2V environments with different velocities.

For IIoT environments, the ability to keep the communication quality in complex multi-path environments is vital for CPS. Since the speed of communication terminals which work in factories and industries always keep in low speed, we set the velocities of terminals in a low level. According to [24], for demonstrating the stability of CPS with channel estimation methods proposed in this paper, we set the parameters for multi-path channel with different number, delay, and power of taps as follows. Some researches pointed out that when the level of radio interference in IIoT environments is very high, the distance between ends is not so far, so in most of the situations, the power of LoS ray is the major component and the Rician channel model is also appropriate for IIoT environments [20]. As the V2V environments, we also adopted the Rician as the fading type in IIoT environments.

Table 3 The mean for BEM-based channel estimation methods in different taps

Number of taps	LS	EKF	UKF
3	0.0574	0.0362	0.0344
6	0.0900	0.0336	0.0326
9	0.1259	0.0355	0.0343
12	0.1548	0.0311	0.0299
15	0.2298	0.0210	0.0200
18	0.4403	0.0362	0.0350

6 Results and discussion

6.1 Simulation results in V2V

In order to demonstate the improvement in robustness and reliability provided by channel estimation methods proposed in this paper, BEM-EKF and BEM-UKF, in end-to-end communication for CPS, we mainly present the performance of them in V2V and IIoT which are the main environments for CPS.

For the V2V environments, we mainly simulate the NMSE and BER in different velocities with a fixed multi-path setting, as the description in Table 3 at first. Since we believe that the channel estimation methods with higher estimation accuracy and lower BERs in different velocities could improve the robustness for end-to-end communication in CPS. On the other hand, we also present the BERs in continuous subframes, which could show the improvement in stability and reliability for CPS. Because the BER is directly correlated with the communication quality, if the BERs keep a stable level in continuous subframes where the speed of terminal is very high, the end-to-end communication in CPS is reliable. Otherwise, if the BERs change obvious from subframe to subframe, we would believe the level of reliability for CPS is in a low level.

Figures 4 and 5 illuminate the BER and NMSE for channel estimation methods in CPS in V2V environments with velocities from 0 to 150 km/h. It could be witnessed in Fig. 4 that the BEM-EKF and the BEM-UKF are still in a

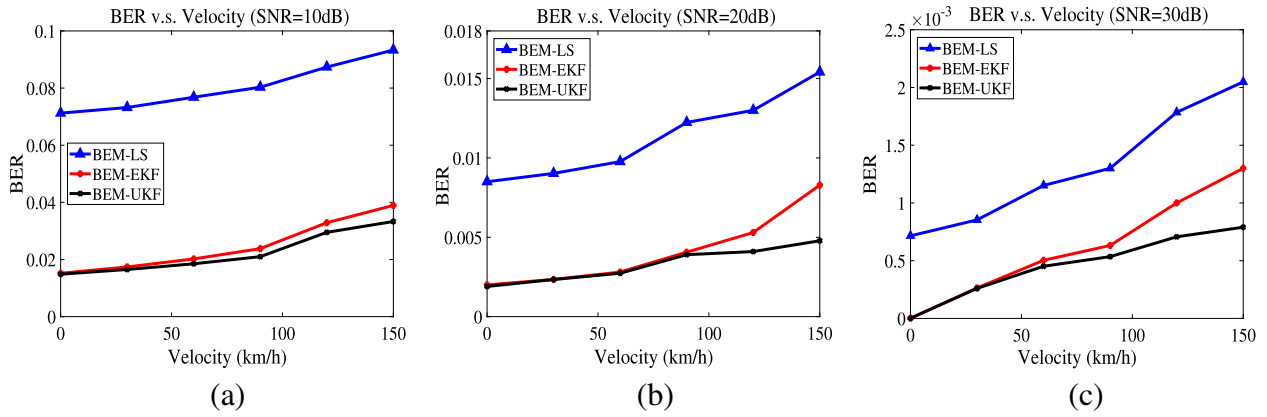

Fig. 4 BER for channel estimation methods in V2V environments with different velocities. BEM-EKF and BEM-UKF are still in a very low level compared with BEM-LS, and with the rising of velocity, BER performance for BEM-LS increases

very low level compared with BEM-LS, and with the rising of velocity, the BER performance for BEM-LS increases from 6×10^{-4} to 2×10^{-3} where the SNR=30 dB as shown in Fig. 4 c, but the BER for BEM-EKF only increases 1.3×10^{-3} and for BEM-UKF, it only rises 0.8×10^{-3}, which demonstrated that the BEM-UKF is very appropriate for the high-speed and non-stationary environments. And Fig. 5 illuminates the same conclusion. We could observe that the NMSE of BEM-EKF and BEM-UKF are nearly one tenth of BEM-LS, because the EKF and UKF could track the change of channel in high velocity environments.

Figure 6 illuminates the BERs change in continuous 100 subframes with different velocities where the SNR=10 dB, and Table V and Table VI present the mean and variance for BEM-LS, BEM-EKF, and BEM-UKF. We could witness that the means of BER of BEM-EKF and BEM-UKF are nearly one third of BEM-LS, and the variance of BEM-EKF and BEM-UKF are also much lower than traditional BEM-LS a lot in all the velocities. It is obvious that the BEM-EKF and BEM-UKF could improve the stability and reliability of CPS.

6.2 Simulation results in IIoT

In the IIoT scenario, dynamic multi-path transmission is an important factor affecting the stability of CPS wireless communication. We set up different delays and attenuations to simulate wireless communication in different multi-path environments, and use the proposed channel estimation methods to simulate the NMSE and BER in different multi-path conditions. As described earlier in this paper, if the NMSE and BER performance obtained by the proposed channel estimation methods can be kept in a stable state in different multi-path conditions, it indicates that the proposed channel estimation methods can

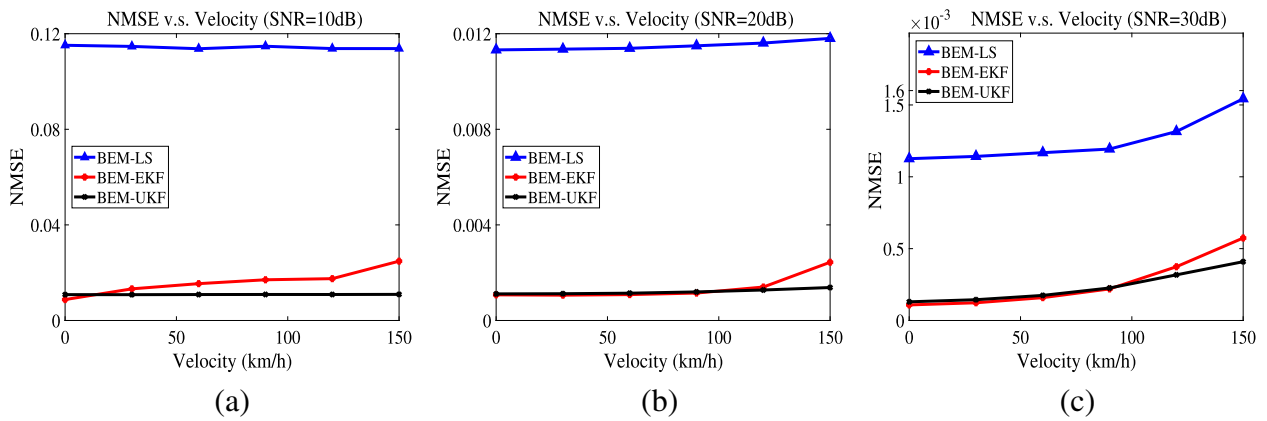

Fig. 5 NMSE for channel estimation methods in V2V environments with different velocities. NMSE of BEM-EKF and BEM-UKF are nearly one tenth of BEM-LS, because the EKF and UKF could track the change of channel in high velocity environments

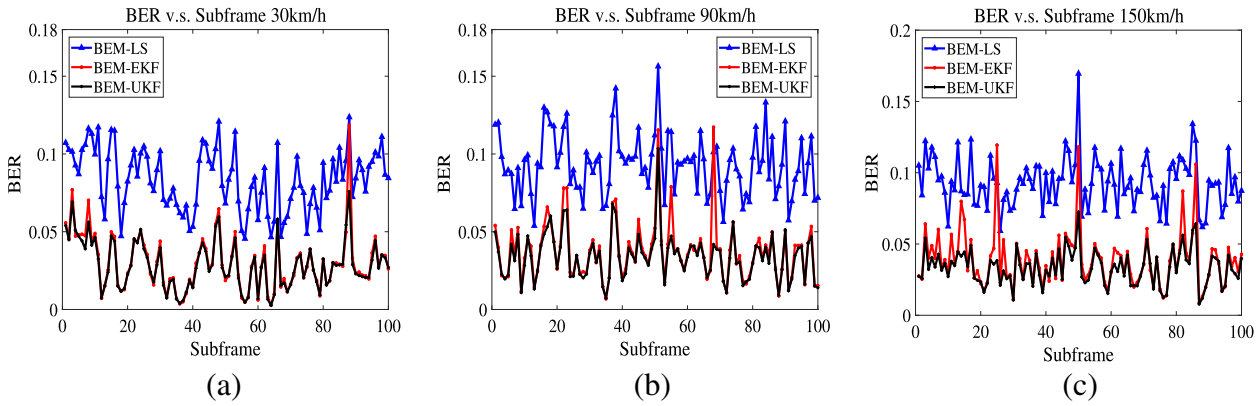

Fig. 6 BER for channel estimation methods in different velocities where the SNR = 10 dB. BERs change in continuous 100 subframes with different velocities. The means of BER of BEM-EKF and BEM-UKF are nearly one third of BEM-LS, and the variance of BEM-EKF and BEM-UKF are also much lower than traditional BEM-LS a lot in all the velocities. It is obvious that the BEM-EKF and BEM-UKF could improve the stability and reliability of CPS

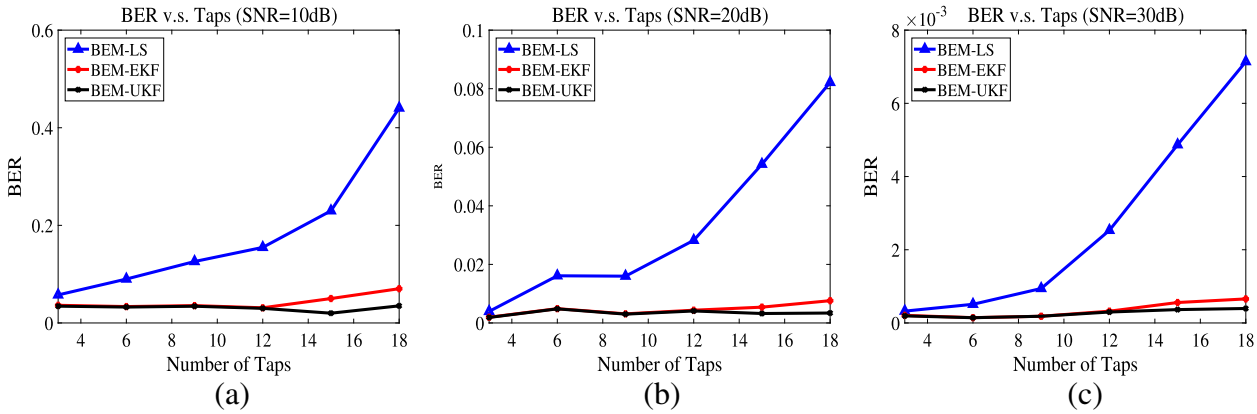

Fig. 7 BER for channel estimation methods in different taps and SNR environments. Under different SNRs, the BER under the BEM-EKF and BEM-UKF channel estimation methods can be stably maintained at a low level with the increase of the number of multi-paths, while the BER has changed a lot under the BEM-LS method

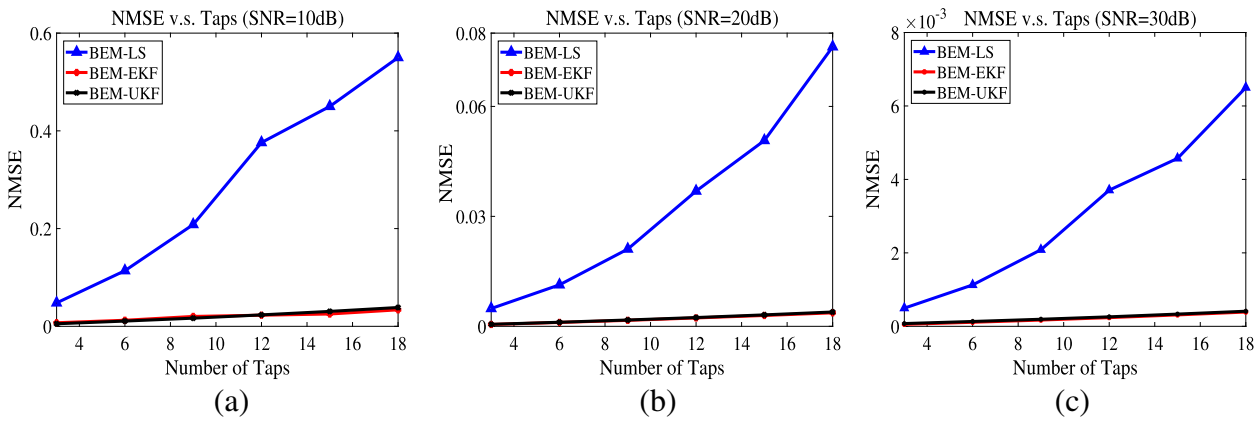

Fig. 8 NMSE for channel estimation methods in different taps and SNR environments. BEM-EKF and BEM-UKF methods can effectively overcome the influence of multi-path fading and improve the stability of CPS wireless communication

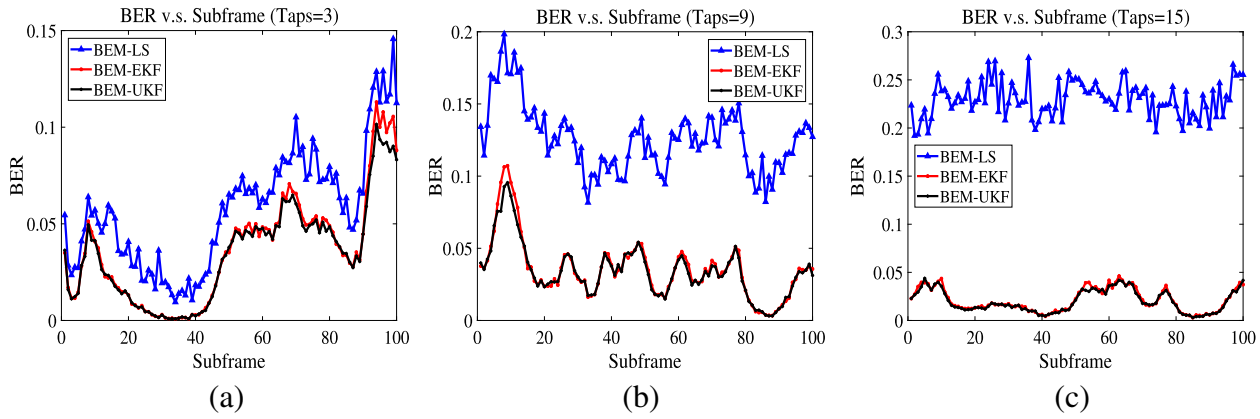

Fig. 9 BER for channel estimation methods in different taps and SNR environments. BER change of 100 consecutive subframes in different multi-path environments where the SNR = 10 dB

improve the robustness of wireless communication of CPS. At the same time, we also simulate the BER variation of consecutive subframes in different multi-path environments to reflect the time domain stability of CPS end-to-end communication.

Figures 7 and 8 show the performances of BER and NMSE for the channel estimation methods in different SNR environments with the taps changed from 3 to 18. From Fig. 7, we can see that under different SNRs, the BER under the BEM-EKF and BEM-UKF channel estimation methods can be stably maintained at a low level with the increase of the number of multi-paths, while the BER has changed a lot under the BEM-LS method. Taking SNR=30 dB as an example, as shown in Fig. 7c, the BER under BEM-EKF and BEM-UKF methods can be kept within 1×10^{-3} in different multi-path conditions. When taps is set to 3, the BER under the BEM-LS method is 3×10^{-4}, and when taps is increased to 18, the BER is increased to 7×10^{-3}. The analysis shows that BEM-EKF and BEM-UKF show better stability in different multi-path conditions, and the performance of the BEM-UKF method is better than that of the BEM-EKF method. The NMSE performance, as shown in Fig. 8, shows the same conclusion, and the BEM-EKF and BEM-UKF methods can effectively overcome the influence of multi-path fading and improve the stability of CPS wireless communication.

Figure 9 reflects the BER change of 100 consecutive subframes in different multi-path environments where the SNR = 10 dB. The mean and variance of the BER obtained by the channel estimation methods of BEM-LS, BEM-EKF, and BEM-UKF are shown in Table VII and Table VIII. According to the results, the BER obtained by the BEM-EKF and BEM-UKF methods is generally lower than the BEM-LS method, and the mean and variance of BER under the BEM-EKF and BEM-UKF methods are smaller than that of the BEM-LS method. Therefore, the BEM-EKF and BEM-UKF methods can be verified to effectively improve the robustness of CPS.

7 Conclusion

In order to ensure reliable and resilient operation of CPS, the end-to-end data transmission must be considered in the communication link with high quality. The main work of this paper is focused on the two important application environments of CPS, including V2V and IIoT. Firstly, we emphasise the importance of channel estimation to enhance the stability of CPS wireless communication and summarize the related work. Then, the doubly selective fading and non-stationary characteristics of V2V and IIoT channels are systematically modeled, the ICI is eliminated through time domain channel estimation, and the complexity of the channel estimation algorithm is further reduced by using BEM. For the non-stationary characteristics of the channel, we use channel estimation and interpolation method based on EKF and UKF to jointly estimate the CIR and time-varying time domain autocorrelation coefficient. At last, the simulation results demonstrate that the BEM-UKF method is able to promote the robustness obviously with high computing, and the BEM-EKF could promote some robustness with lower computing. It is no doubt that the BEM-based Bayesian filter channel estimation methods are appropriate for robust and reliable end-to-end communication of V2V and IIoT.

Our future work will study the actual channel conditions for V2V and IIoT to extract key parameters from actual channel data and complete actual channel modeling, thus improving the availability of channel estimation algorithms in practical applications.

Abbreviations
CPSs: Cyber-physical systems; V2V: Vehicle-to-vehicle; ICI: Intercarrier interference; BEM: Basis extended model; EKF: Extended Kalman filter; UKF: Unscented Kalman filter; CIR: Channel impulse response; 3C: Communication and control technologies; NMSE: Normalized minimum mean error; OFDM: Orthogonal Frequency Division Multiplexing; CDP: Constructed data pilots; GRMP: Gradient Rake-Matching Pursuit Algorithm; FA-TT: Finite Alphabet with Time Truncation; MD-TT: Minimum Distance with Time Truncation; DD-TT: Decision Directed with Time Truncation; TDL: Tapped delay line; DoA: Direction of arrival

Funding
This work was supported by the National Natural Science Foundation of China (No. 61501066), Chongqing Frontier and Applied Basic Research Project (No. cstc2015jcyjA40003), Graduate Research and Innovation Foundation of Chongqing, China (No. CYS18061), and the Fundamental Research Funds for the Central Universities (No. 106112017CDJXY500001).

Availability of data and materials
The authors do not share the data, due to the requirements of the foundations.

Authors' contributions
YL contributed on the design of the methods on the EKF/UKF-based channel estimation. XS and GS presented the performance evaluation. XD and SW participated in the design and optimization of the framework. All authors have read and approved the final manuscript.

Competing interests
The authors declare that they have no competing interests.

Publisher's Note

Author details
[1]Center of Communication and TT&C, Chongqing University, Chongqing, China. [2]Faculty of Engineering and Environment, Northumbria University, Newcastle upon Tyne, UK. [3]School of Information and Safety Engineering, Zhongnan University of Economics and Law, Wuhan 430073, China.

Received: 7 February 2019 Accepted: 3 April 2019
Published online: 03 June 2019

References
1. X. Xu, Y. Xue, L. Qi, Y. Yuan, X. Zhang, T. Umer, S. Wan, An edge computing-enabled computation offloading method with privacy preservation for internet of connected vehicles. Futur. Gener. Comput. Syst. **96**, 89–100 (2019)
2. F. U. Din, A. Ahmad, H. Ullah, A. Khan, T. Umer, S. Wan, Efficient sizing and placement of distributed generators in cyber-Physical power systems. J. Syst. Archit. (2019). https://doi.org/10.1016/j.sysarc.2018.12.004
3. A. L. Edward, in *Proc. the 47th Design Automation Conference on - DAC*. CPS foundations (IEEE, Anaheim, 2010), pp. 737–742
4. S. K. Khaitan, J. D. Mccalley, Design techniques and applications of cyber physical systems: a survey. IEEE Syst. J. **9**(2), 350-365 (2015)
5. D. Jia, K. Lu, J. Wang, X. Zhang, X. Shen, A survey on platoon-based vehicular cyber-physical systems. IEEE Commun. Surv. Tutor. **18**(1), 263–284 (2016)
6. S. Wan, Y. Zhao, T. Wang, Z. Gu, Q. H. Abbasi, K. K. R. Choo, Multi-dimensional data indexing and range query processing via Voronoi diagram for Internet of Things. Futur. Gener. Comput. Syst. **91**, 382–391 (2019)
7. M. Haferkamp, B. Sliwa, C. Ide, C. Wietfeld, in *Proc. Wireless Days*. Payload-Size and Deadline-aware scheduling for time-critical Cyber Physical Systems (IEEE, Porto, 2017), pp. 4–7
8. B. M. Lee, H. Yang, Massive MIMO for industrial internet of things in cyber-physical systems. IEEE Trans. Ind. Inform. **14**(6), 2641–2652 (2017)
9. Y. Liu, Z. Tan, H. Hu, L. Cimini, Channel estimation for OFDM. IEEE Commun. Surv. Tutor. **16**(4), 1891–1908 (2014)
10. C. Wang, A. Ghazal, B. Ai, Y. Liu, Channel measurements and models for high-speed train communication systems: a survey. IEEE Commun. Surv. Tutor. **18**(2), 974–987 (2016)
11. X. Li, J. Peng, J. Niu, F. Wu, J. Liao, K. R. Choo, A robust and energy efficient authentication protocol for Industrial Internet of Things. IEEE Int. Things J. **5**(3), 1606–1615 (2017)
12. X. Cheng, Q. Yao, M. Wen, C. X. Wang, L. Song, B. Jiao, Wideband channel modeling and ICI cancellation for vehicle-to-vehicle communication systems. IEEE J. Sel. Areas Commun. **31**(9), 434–448 (2013)
13. Y. Liao, X. Shen, X. Dai, M. Xhao, D. Li, X. Zhou, in *Proc. IEEE Global Communication Conference*. EKF-based joint channel estimation and decoding design for non-stationary OFDM channel (IEEE, Singapore, 2017), pp. 1–6
14. C. X. Wang, X. Cheng, D. I. Laurenson, Vehicle-to-vehicle channel modeling and measurements: recent advances and future challenges. IEEE Commun. Mag. **47**(11), 96–103 (2009)
15. A. F. Molisch, F. Tufvesson, J. Karedal, C. F. Mecklenbrauker, A survey on vehicle-to-vehicle propagation channels. IEEE Wirel. Commun. **16**(6), 12–22 (2009)
16. M. S. Hossen, M. S. Bang, Y. Park, K. D. Kim, in *Proc. IEEE International Conf on Ubiquitous & Future Networks*. Performance analysis of an OFDM-based method for V2X communication (IEEE, Shanghai, 2014), pp. 238–242
17. M. Walter, D. Shutin, A. Dammann, Time-variant doppler PDFs and characteristic functions for the vehicle-to-vehicle channel. IEEE Trans. Veh. Technol. **66**(12), 10748–10763 (2017)
18. A. Borhani, M. Tzold, in *Proc. IEEE Vehicular Technology Conference*. Modeling of vehicle-to-vehicle channels in the presence of moving scatterers (IEEE, Quebec City, 2012), pp. 1–5
19. Z. Zhao, X. Cheng, M. Wen, B. Jiao, Channel estimation schemes for IEEE 802.11p standard. IEEE Intell. Transp. Syst. Mag. **5**(4), 38–49 (2013)
20. K. Chelli, P. Sirsi, T. Herfet, in *Proc. IEEE International Conference on Consumer Electronics*. Complexity reduction for consumer device compressed sensing channel estimation (IEEE, Boston, 2017), pp. 189–194
21. M. M. Awad, K. G. Seddik, A. Elezabi, in *Proc. IEEE Vehicular Technology Conference*. Channel estimation and tracking algorithms for harsh vehicle to vehicle environments (IEEE, Berlin, 2015), pp. 1–5
22. M. Sybis, in *Proc. IEEE International Conference on Connected Vehicles and Expo*. Channel estimation with two-dimensional interpolation for the 802.11p communication (IEEE, Vienna, 2014), pp. 693–694
23. L. D. Xu, W. He, S. Li, Internet of Things in industries: a survey. IEEE Trans. Ind. Informa. **10**(4), 2233–2243 (2014)
24. M. Cheffena, Propagation channel characteristics of industrial wireless sensor networks [wireless corner]. IEEE Antennas Propag. Mag. **58**(1), 66–73 (2016)
25. T. S. Rappaport, C. D. Mcgillem, UHF fading in factories,. IEEE J. Sel. Areas Commun. **7**(1), 40–48 (1989)
26. E. Tanghe, W. Joseph, L. Verloock, L. Martens, The industrial indoor channel: large-scale and temporal fading at 900, 2400, and 5200 MHz. IEEE Trans. Wirel. Commun. **7**(7), 2740-2751 (2008)
27. E. Vinogradov, W. Joseph, C. Oestges, Measurement-based modeling of time-variant fading statistics in indoor peer-to-peer scenarios. IEEE Trans. Antennas Propag. **63**(5), 2252–2263 (2015)
28. P. Schniter, S. J. Hwang, S. Das, A. P. Kannu, Equalization of time-varying channels. Int. J. Adapt. Control Sig. Process. **22**(7), 705–716 (2010)
29. K. Chelli, T. Herfet, in *Proc. IEEE International Conference on Computer and Communications*. Doppler shift compensation in vehicular communication systems (IEEE, Chengdu, 2017), pp. 2188–2192
30. J. Gozalvez, M. Sepulcre, R. Bauza, IEEE 802.11p vehicle to infrastructure communications in urban environments,. IEEE Commun. Mag. **50**(5), 176–183 (2012)
31. B. Wu, M. D. Lemmon, H. Lin, Formal methods for stability analysis of networked control systems with IEEE 802.15.4 protocol. IEEE Trans. Cont. Syst. Technol. **PP**(99), 1-11 (2017)
32. F. Hlawatsch, G. Matz, *Wireless communications over rapidly time-varying channels*. (Academic Press, USA, 2011)
33. E. Simon, M. Khalighi, Iterative soft-Kalman channel estimation for fast time-varying MIMO-OFDM channels. IEEE Wirel. Commun. Lett. **2**(6), 599-602 (2013)
34. S. Srkk, *Bayesian filtering and smoothing*. (Cambridge University Press, USA, 2013)
35. S. Sesia, I. Toufik, M. Baker, *LTE–the UMTS long term evolution: from theory to practice*. (Wiley Publishing, USA, 2009)
36. X. Dai, W. Zhang, J. Xu, J. E. Mitchell, Y. Yang, Kalman interpolation filter for channel estimation of LTE downlink in highmobility environments. EURASIP J. Wirel. Commun. Netw. **2012**(1), 232–246 (2012)